Dual-Band Evanescent-Mode Substrate Integrated Waveguide Band-pass Filter for WLAN Applications

Amir Nosrati and Mahmud Mohammad-Taheri
School of Electrical and Computer Engineering, College of Engineering, University of Tehran, Tehran, Iran
amirnosrati@ut.ac.ir, mtaheri@ut.ac.ir
Corresponding author: Mahmud Mohammad-Taheri

***Abstract*- A new multi-layer substrate integrated waveguide (SIW) structure is developed to design dual-band evanescent-mode band-pass filters (BPFs). Two independent series *LC* circuits are implemented by incorporating metallic irises in the different layers of the structure. The combination of the metallic irises with capacitive-plates is embedded inside the SIW to independently excite two evanescent-mode resonance frequencies below the cut-off frequency of the structure. Two integrated series irises and capacitive-plates are incorporated in an antipodal configuration to minimize the coupling interference between them. A dual-band evanescent-mode band-pass filter is designed and characterized at 2.4GHz and 5.8GHz frequencies for Wireless Local Area Network (WLAN). The first resonance frequency of the filter is fixed at 2.4GHz (2400-2484MHz) and the second one is tuned at 5.2GHz (5150-5350MHz) to partially meet the standard IEEE 802.11 WLAN bandwidths and fully meet the WLAN frequencies. This approach demonstrates the miniaturized dual-band high quality- factor evanescent-mode band-pass filter. The structure is designed and simulated by taking into account of all fabrication aspects.**

***Index Terms*-** Band-pass filter (BPF), capacitive-plate, evanescent-mode, substrate integrated waveguide (SIW), wireless local area network (WLAN).

I. INTRODUCTION

Evanescent-mode technique is capable to simultaneously demonstrate high quality-factor and miniaturized size structures which required for wireless communication systems as well as environmental sensors and biomedical applicators [2]-[7]. This technique is mainly reported to design single-band microwave devices, while there are a few structures for dual-band BPFs but at the expense of lower quality-factor and/or larger area size [8]-[10]. For instance, the metamaterial-based dual-band evanescent-mode filter is reported to sacrifice quality-factor in favor of dual functionality [9]. Moreover, another band-pass filter is proposed to excite the second evanescent-mode

Manuscript received 5-Aug.-2019 and revised 18-Nov.-2019,
Accepted on 21- December-2019
P- ISSN: 2322-4088
E- ISSN: 2322-3936

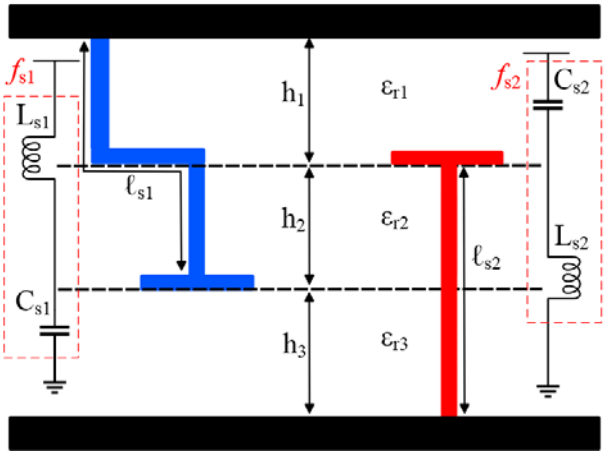

Fig. 1. Cross-section (side view) of the developed three-layer SIW with two antipodal series-connected iris and capacitive-plate circuits.

pole using a series *LC* circuit in the propagation direction but at the expense of lower quality- factor [10]. Inspecting the design procedure for the conventional single-band evanescent-mode filters shows that the operation principle is based on incorporating a series metallic iris integrating with a capacitive-plate in the transverse direction inside a 3D waveguide structure [11]. The primary design procedure for dual-band BPF is the incorporation of two individual series-connected circuits of the metallic iris and capacitive-plate configuration in the transverse direction. However, this configuration results in a single-band evanescent-mode filter in which the total inductance and capacitance of the two circuits operate at a single resonance frequency due to the same resonance frequencies of the metallic irises and capacitive-plates located at the same heights (same wavelengths). To design a dual-band evanescent-mode BPF, two SIWs with different thicknesses are stacked to realize the three-layer structure. Two series metallic irises integrated with two capacitive-plates are vertically incorporated inside the SIW structure in an antipodal configuration. The structure generates two independent resonance frequencies. The developed structure is reported to preserve high quality-factor as well as the compactness of the structure.

II. DESIGN OF DUAL-BAND EVANESCENT-MODE BPF

Fig. 1 shows a schematic cross-section of the proposed structure in which two series metallic irises integrated with two capacitive-plates are vertically incorporated inside the SIW structure in an antipodal configuration. The three-layer structure enables the design to realize two irises with different physical and/or electrical lengths. These two irises with different electrical lengths represent two inductors with different characteristics. Therefore, two series *LC* resonators with different resonance frequencies can be realized by the integration of the two irises with the same capacitor. As

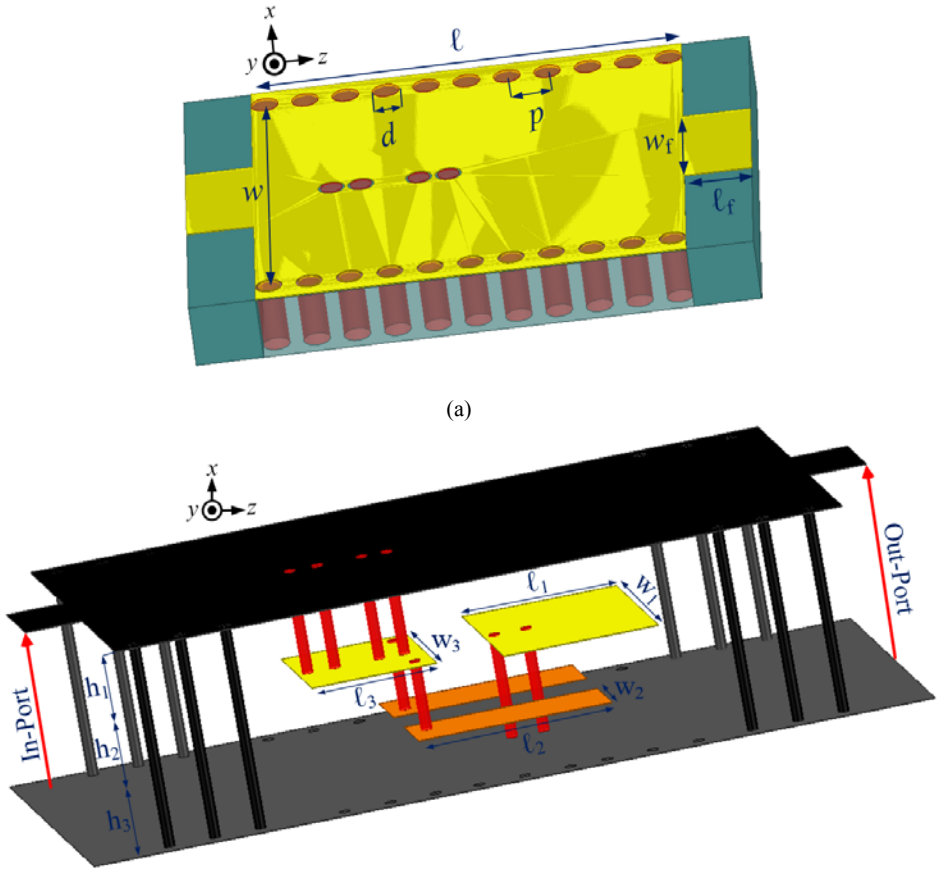

Fig. 2. (a) 3D view of the structure consisting of a SIW part and two microstrip transitions. (b) Schematic diagram of the triple-layer SIW BPF depicting the critical dimensions of the capacitive-plates (the opening on the right and left sides of the structure is merely for visualization purposes).

can be seen from Fig. 1, the first series-connected iris and the capacitive-plate realizes the L_{s1}-C_{s1} circuit has the resonance frequency of f_{s1} while the combination of the second iris and capacitive-plate realizes the L_{s2}-C_{s2} circuit has a different resonance frequency of f_{s2} [12]. The structure adds a degree of freedom by which the lengths of the two irises are chosen to be equal, whereas the two capacitive-plates can have different dimensions to generate different resonant frequencies. Based on the developed structure, a dual-band evanescent-mode BPF is designed in two modes with the resonance frequencies of f_{s1}=2.46GHz, f_{s2} =5.74GHz, and f_{s1}=2.44GHz, f_{s2} =5.26GHz as shown in Fig. 4 and Fig. 6, respectively for WLAN applications. Fig. 1 shows the structure of the filter simulated on a three-layer substrate with heights of h_1=h_2=h_3=0.508mm. Rogers RT/duroid 5880 with a dielectric constant and loss tangent of ε_r=2.2 and tanδ=0.0009, respectively, are used for the substrate. To fulfill the manufacturing requirements, the thickness of the soldering parts is considered to be 35μm. The parameters of the structure are optimized to realize two independent resonance frequencies. Fig. 3 shows the 2D sketch (top view) of the structure as well as the optimized dimensions. The effective

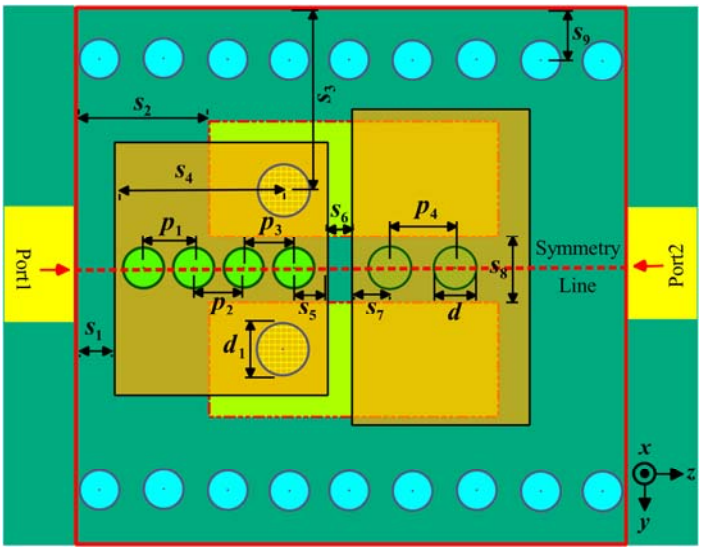

Fig. 3. 2D sketch (top view) of the proposed BPF with optimized values of ℓ=16mm, w= 15mm, ℓ_f=2.5mm, w_f=4.9mm, w_2=3.8mm, ℓ_3=5.5mm, d=1mm, d_1=1.2mm, p=1.5mm, p_3=1.1mm, s_1=2.3mm, s_2=5mm, s_5=0.55mm, s_6=0.2mm, s_7=0.7mm, s_8=1.2mm, and s_9=1mm.

width, via hole and pitch are calculated using the design considerations in [13].

From (1) and (2) in [13], given the w=15mm, d=1mm, and p=1.5mm, the cut-off frequency of the structure is calculated to be around 7.1GHz.

$$w_{eff} = w - 1.08\frac{d^2}{p} + 0.1\frac{d^2}{w} \tag{1}$$

$$f_c = \frac{C_0}{2w_{eff}\sqrt{\varepsilon_r}} \tag{2}$$

As can be seen from Fig. 2 and Fig. 3, the filtering structure is fed by two non-tapered 50Ω microstrip lines. Equation (3) is employed to calculate the width of the 50Ω feed lines [1].

Given the dielectric constant of ε_r=2.2 and total substrate thickness of h=1.524mm, the width of the feed lines is calculated to be around w_f=4.9mm.

$$\frac{w_f}{h} = \begin{cases} \dfrac{8e^A}{e^{2A}-2} & for\ \dfrac{w_f}{h} \le 1 \\ \dfrac{2}{\pi}\left[B - 1 - \ln(2B-1) + \dfrac{\varepsilon_r - 1}{2\varepsilon_r}\left(\ln(B-1) + 0.39 - \dfrac{0.61}{\varepsilon_r}\right)\right] & for\ \dfrac{w_f}{h} \ge 1 \end{cases} \tag{3}$$

$$A = \frac{Z_c}{60}\sqrt{\frac{\varepsilon_r + 1}{2}} + \frac{\varepsilon_r - 1}{\varepsilon_r + 1}\left(0.23 + \frac{0.11}{\varepsilon_r}\right), \quad B = \frac{377\pi}{2Z_c\sqrt{\varepsilon_r}} \tag{4}$$

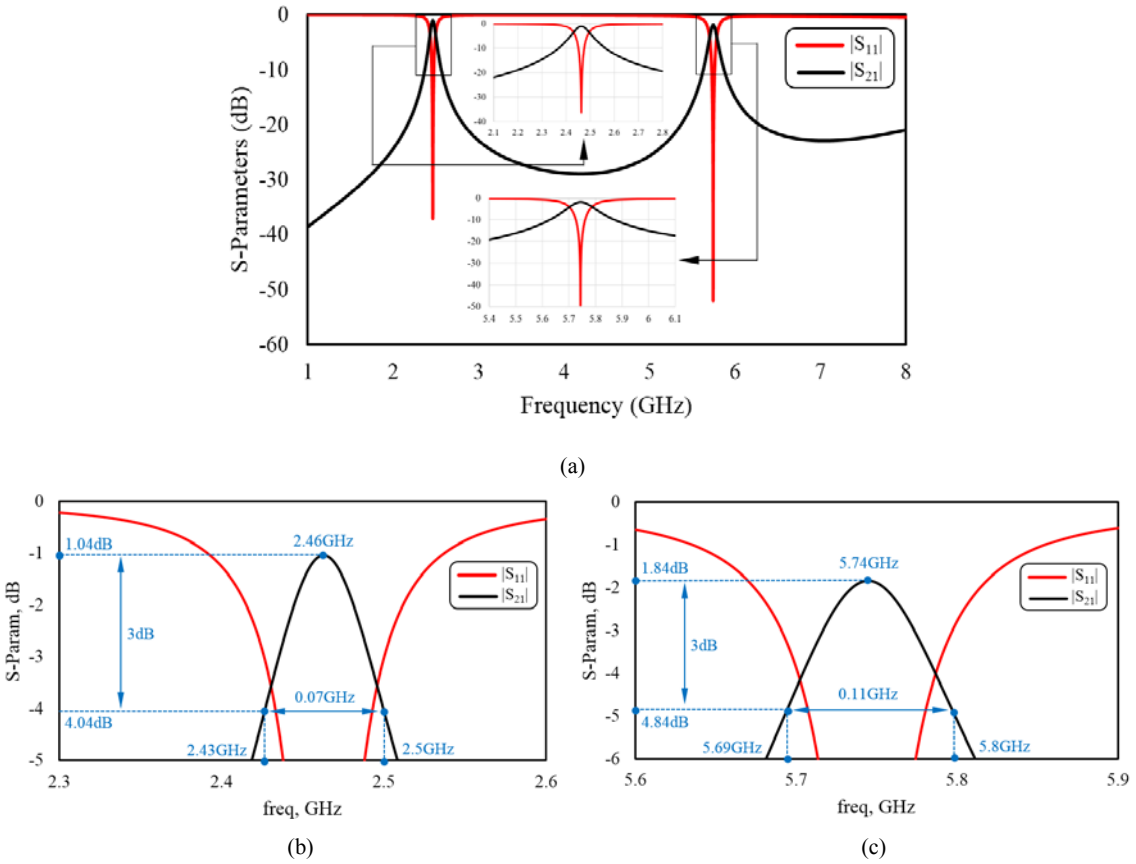

Fig. 4. (a) EM-simulated S-parameters of the proposed dual-band evanescent-mode BPF with optimized parameters of ℓ_1=5.3mm, w_1=10mm, ℓ_2=8.1mm, w_3=5mm, s_3=8.5mm, s_4=4.8mm, p_1=1.1mm, p_2=2.15mm, and p_4=1.2mm. (b) Lower pass-band and (c) upper pass-band in detail.

III. SIMULATED RESULTS

A dual-band evanescent-mode BPF is designed and simulated with the optimized parameters in Fig. 3.The filter is reported to demonstrate two resonance frequencies at f_{s1}=2.46GHz and f_{s2}=5.74GHz (below the cut-off frequency at f_c=7.1GHz) with the fractional bandwidths of FBW_1=2.85% which is close to full FBW of the lower band and FBW_2=1.92%, which partially fulfills the bandwidth requirement in 5.8 GHz band, respectively. The bandwidth can be further improved by introducing more loss in the filter structure which is out of the scope of this paper as the main focus has been on miniaturization of the structure. The insertion and return losses are better than 1.04dB, 20dB for the lower-band while are 1.84dB and 20dB for the upper-band, respectively. To evaluate the two independent resonance frequencies, the first band is determined to be fixed while the second band is tuned for several different values. The resonance frequency of f_{s2} can be tuned by changing the length of the iris or the dimension of the capacitive-plate in the circuit. Fig. 5 shows the EM-simulated results for four different values of this parameter. The results represent four different resonance

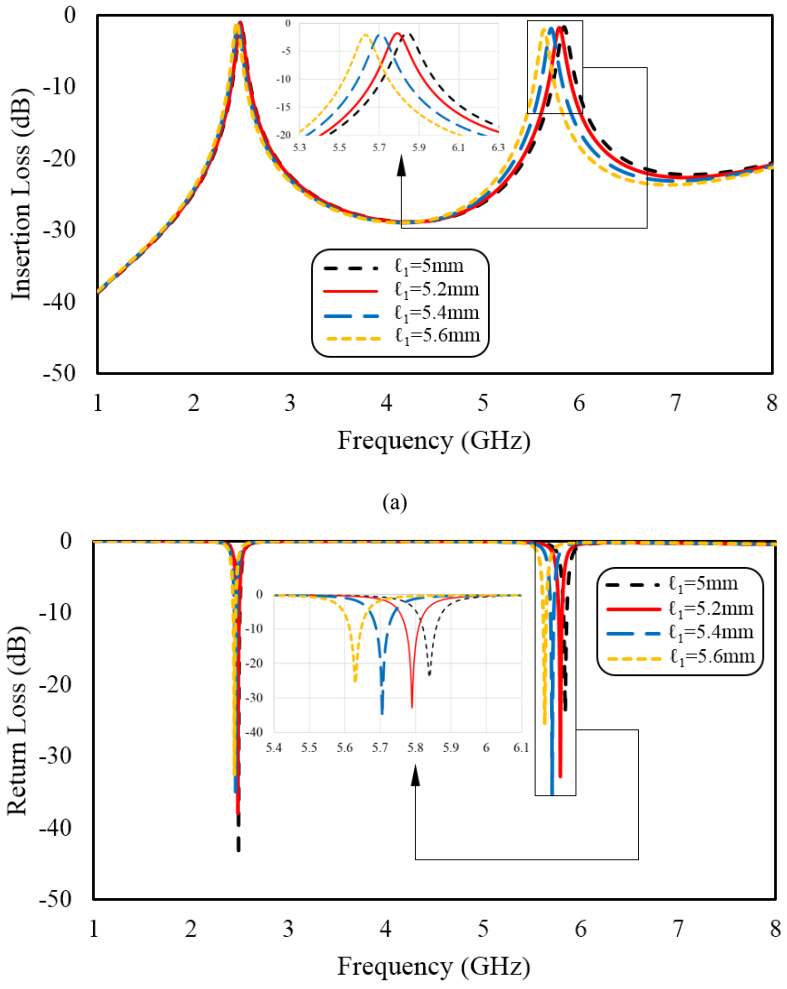

Fig. 5. Simulated results for four different values of ℓ_1 parameter equal to 5mm, 5.2mm, 5.4mm, and 5.6mm with four different resonance frequencies of 5.84GHz (IL=1.69dB, RL=24dB, FBW=1.88%), 5.79GHz (IL=1.78dB, RL=32.9dB, FBW=1.73%), 5.71GHz (IL=1.91dB, RL=35.4dB, FBW=1.75%), and 5.63GHz (IL=2.07dB, RL=25.7dB, FBW=1.78%), respectively. (a) $|S_{21}|$ and (b) $|S_{11}|$.

frequencies of 5.84GHz, 5.79GHz, 5.7GHz, and 5.63GHz for four different values of ℓ_1 equal to 5mm, 5.2mm, 5.4mm, and 5.6mm, respectively. It can be shown that the second resonance frequency can be further tuned by changing the dimensions of the capacitive-plates where the relation between physical dimensions and the corresponding lumped-element circuit and, consequently, the resonance frequency of the structure has been discussed in detail in [12]. To cover the 5.2 GHz band, the structure is simulated and optimized, where the scattering parameters are shown in Fig. 6. The insertion loss at three different resonance frequencies of 5.4GHz, 5.32GHz, and 5.2GHz for three different values of ℓ_1 equal to 6.4 mm, 6.6 mm, and 7 mm, respectively, are shown in Fig. 7, in which the lower resonance frequency fixed.

Table I. The parameters of the proposed dual-band evanescent-mode BPF

Bands	[2.4-5.2] GHz		[2.4-5.8] GHz	
f_0 (GHz)	2.44	5.26	2.46	5.74
Return Loss (dB)	47.8	31.3	37	52.1
Insertion Loss (dB)	1.02	1.88	1.04	1.84
$f_{cut\text{-}off}$ (GHz)	7.1		7.1	
Dim. ($\lambda \times \lambda$)*	0.19×0.20		0.19×0.20	
FBW (%)	3.28	1.9	2.85	1.92

* λ is the wavelength related to the center frequency of the lower-band in the medium.

Table II. Comparison between the parameters of the proposed dual-band SIW BPF with those of other references

BPF	Dim. ($\lambda \times \lambda$)	f_0 (GHz)		FBW (%)		IL (dB)	
[5]	0.93×0.88	30.3	39.3	4.5	4.1	3.8	3.8
[8]	0.12×0.42	6.2	10	19.3	13	1	1
[9]	0.2×0.19	4.05	5.8	4.59	3.58	2.25	2.25
[10]	0.16×0.16	1.89	3.76	5.4	2.8	2.3	2
[12]	0.36×0.33	1.5	3	6.6	3.3	1	4.6
New*	0.2×0.19	2.46	5.74	2.85	1.92	1.04	1.84

* Proposed structure.

Two other conventional commercial softwares (Agilent ADS and CST Microwave Studio) are employed to regenerate the simulated results generated by Ansys HFSS to show the validity of our proposed method. As can be seen in Fig. 8, the simulated S-parameters obtained by our proposed method are in good agreement with other well-known microwave softwares.

The designed dual-band evanescent-mode BPF can be fabricated on a three-layer substrate integrated waveguide with the common PCB technology. The main concern in the fabrication is the use of material with the same dielectric constant between the layers to attach them in the case of using common PCB technologies.

It should be noted that the developed structure adds further complexity in the fabrication of the filter. For instance, the developed structure is realizable on a three-layer substrate integrated waveguide structure while the filter in [12] have been realized on a two-layer SIW. While adding an extra layer can contribute to size reduction, it increases the structural complexity and the insertion loss due to adding extra dielectric between the layers to attach them together.

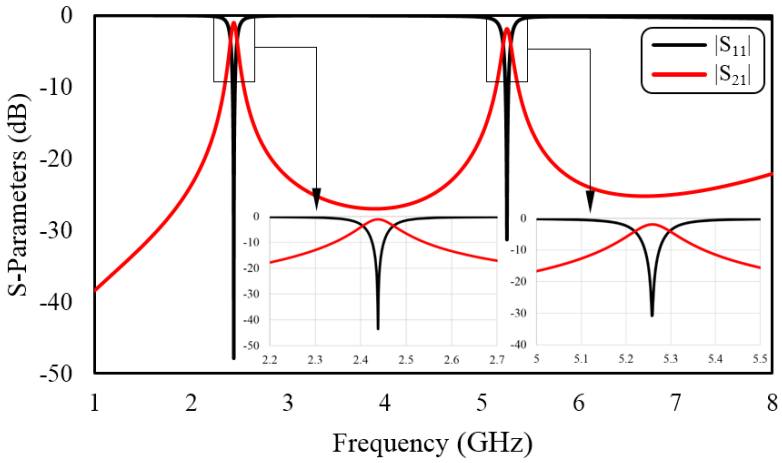

(a)

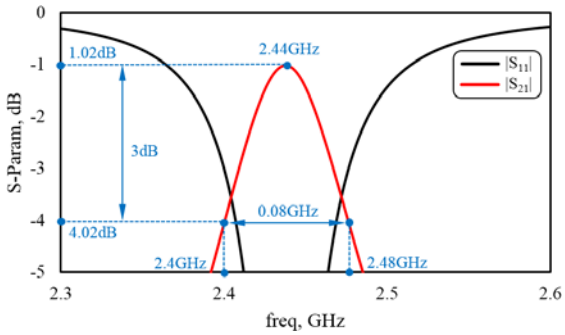

(b)

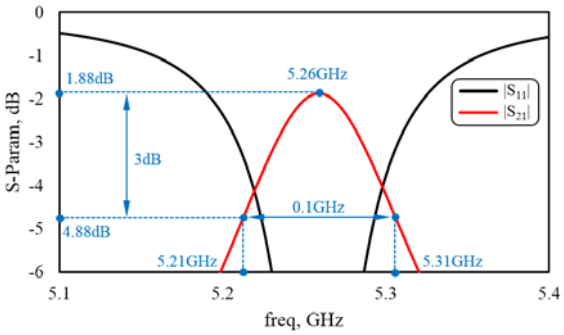

(c)

Fig. 6. (a) EM-simulated results with optimized values of ℓ_1=6.8mm, w_1=9mm, ℓ_2=8.3mm, s_3=7mm, s_4=4.3mm, p_1=1.2mm, p_2=2.05mm, and p_4=1.4mm. There are two pass-bands below the cut-off frequency of the SIW at 2.44GHz (IL=1.02dB, RL=47.8dB, FBW=3.28%) and 5.26GHz (IL=1.88dB, RL=31.3dB, FBW=1.9%). Close up view of the (b) lower pass-band and (b) upper pass-band.

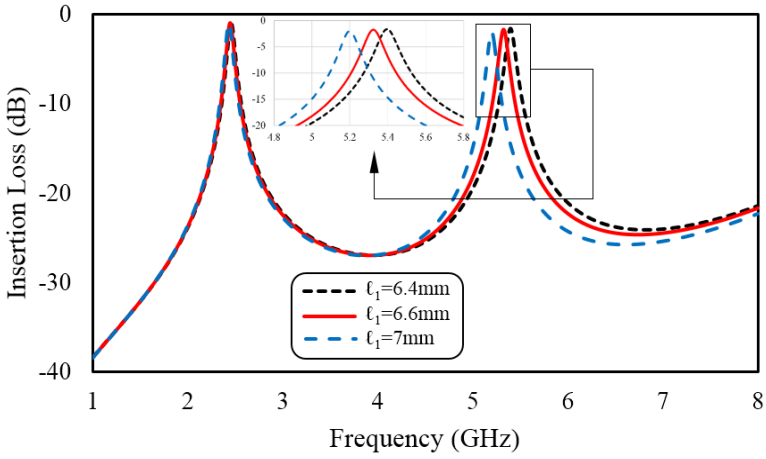

(a)

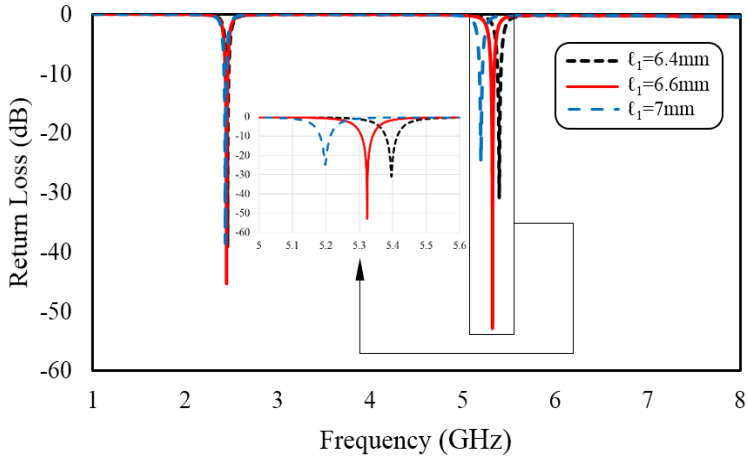

(b)

Fig. 7. EM-simulated scattering parameters for three different values of ℓ_1 parameter equal to 6.4mm, 6.6mm, and 7mm with three different resonance frequencies of 5.4GHz (IL=1.64dB, RL=31dB, FBW=1.85%), 5.32GHz (IL=1.75dB, RL=52.6dB, FBW=1.88%), and 5.2GHz (IL=2.02dB, RL=24.8dB, FBW=1.92%), respectively. (a) $|S_{21}|$ and (b) $|S_{11}|$.

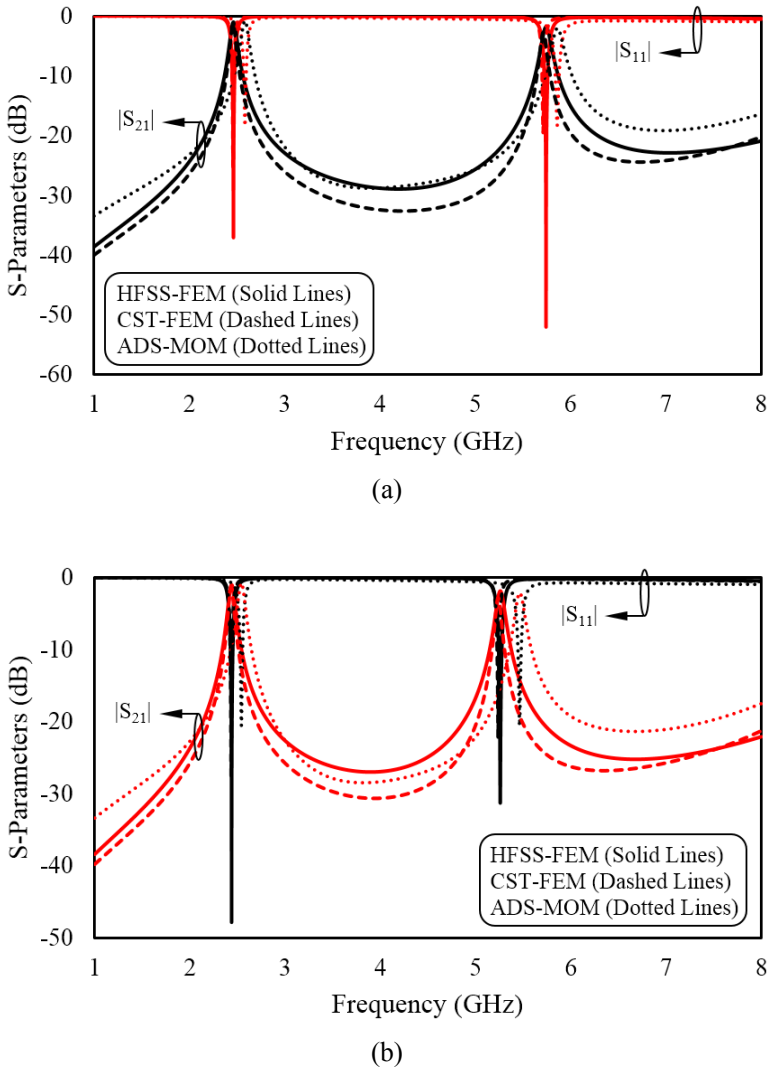

Fig. 8. Comparison between EM-simulated results generated by three commercial softwares, Ansys HFSS, CST Microwave Studio, and Agilent ADS. (a) [2.4-5.8] bands and (b) [2.4-5.2] bands.

IV. CONCLUSION

A new multi-layer substrate integrated waveguide (SIW) structure has been developed and characterized for dual-band evanescent-mode band-pass filters (BPFs) realization. It has been shown that the integration of two sets of the metallic irises with capacitive-plates in an antipodal configuration inside the SIW can excite two independent evanescent-mode resonance frequencies below the SIW cut-off frequency. Based on the developed configuration, a dual-band evanescent-

mode band-pass filter has been designed to operate at 2.4GHz and 5.8GHz frequencies for Wireless Local Area Network (WLAN). The first resonance frequency of the filter has been reported to be fixed, while the second resonant frequency can be tuned at 5.2GHz to meet the standard IEEE 802.11 WLAN frequencies. Miniaturized dual-band high quality-factor evanescent-mode band-pass filter was demonstrated by the proposed approach.

ACKNOWLEDGMENT

The authors would like to thank Dr. Mehdi Nosrati, university of McGill, for his constructive collaboration and useful comments.

REFERENCES

[1] D. M. Pozar, *Microwave Engineering*, 3rd ed. New York, NY, USA: Wiley, 2005.

[2] H. Joshi, H. H. Sigmarsson, S. Moon, D. Peroulis, and W. J. Chappell, "High-Q fully reconfigurable tunable bandpass filters," *IEEE Trans. Microw. Theory Techn*, vol. 57, no. 12, pp. 3525-3533, Dec. 2009.

[3] Y. D. Dong, T. Yang, and T. Itoh, "Substrate integrated waveguide loaded by complementary split-ring resonators and its application to miniaturized waveguide filters," *IEEE Trans. Microw. Theory Tech*., vol. 57, no. 9, pp. 2211-2223, Sep. 2009.

[4] S. Bastioli and R. V. Snyder, "Broad passband, wide stopband, high power evanescent mode filters using capacitively-loaded ridges," *in Proc. 42nd Eur. Microw. Conf., (EuMC),* Nov. 2012, pp. 176-179.

[5] B.-J. Chen, T.-M. Shen, and R.-B. Wu, "Dual-band vertically stacked laminated waveguide filter design in LTCC technology," *IEEE Trans.Microw. Theory Tech.*, vol. 57, no. 6, pp. 1554-1562, June 2009.

[6] S.-J. Park, I. Reines, C. Patel, and G. M. Rebeiz, "High-Q RF-MEMS 4–6 GHz tunable evanescent-mode cavity filter," *IEEE Trans. Microw. Theory Tech.*, vol. 58, no. 2, pp. 381-389, Feb. 2010.

[7] D. Vrba, J. Vrba, O. Fiser, I. Merunka, J. Cumana, J. Vrba, "Perspective applications of microwaves in medicine," *28th IEEE Conf. Radio elctronica*, June 2018.

[8] T. Yan and X.-H. Tang, "Substrate integrated waveguide dual-band bandpass filter with complementary modified split-ring resonators," *in Proc. IEEE Int. Wireless Symp. (IWS)*, Apr. 2015, pp. 1-4.

[9] Y. Dong and T. Itoh, "Miniaturized dual-band substrate integrated waveguide filters using complementary split-ring resonators," *in IEEE MTT-S Int. Microw. Symp. Dig*., June 2011, pp. 1-4.

[10] M. Nosrati and M. Daneshmand, "Gap-coupled excitation for evanescent-mode substrate integrated waveguide filters," *IEEE Trans. Microw. Theory Tech*., vol. 66, no. 6, pp. 3028-3035, June 2018.

[11] G. F. Craven and C. K. Mok, "The design of evanescent mode waveguide bandpass filters for a prescribed insertion loss characteristic," *IEEE Trans. Microw. Theory Tech.,* vol. vol. 19, no. 3, pp. 295-308, Mar. 1971.

[12] M. Nosrati and M. Daneshmand, "Substrate integrated waveguide L-shaped iris for realization of transmission zero and evanescent-mode pole," *IEEE Trans. Microw. Theory Tech*., vol. 65, no. 7, pp. 2310-2320, July 2017.

[13] F. Xu and K. Wu, "Guided-wave and leakage characteristics of substrate integrated waveguide," *IEEE Trans. Microw. Theory Tech.*, vol. 53, no. 1, pp. 66-73, Jan. 2005.

L.-S. Wu, X.-L. Zhou, W.-Y. Yin, L. Zhou, and J.-F. Mao, "A substrate integrated evanescent-mode waveguide filter with nonresonating node in low-temperature co-fired ceramic," *IEEE Trans. Microw. Theory Tech*., vol. 58, no. 10, pp. 2654-2662, Oct. 2010.